Exploring the Role of the Active Site Cysteine in Human Muscle Creatine Kinase†

Pan-Fen Wang,‡ Allen J. Flynn,‡ Mor M. Naor,§,|| Jan H. Jensen,§ Guanglei Cui,⊥ Kenneth M. Merz, Jr.,⊥ George L. Kenyon,‡ and Michael J. McLeish*,‡

Department of Medicinal Chemistry, University of Michigan, 428 Church Street, Ann Arbor, Michigan 48109, Department of Chemistry, University of Iowa, Iowa City, Iowa 52242, and Department of Chemistry and the Quantum Theory Project, University of Florida, Gainesville, Florida 32611

Received April 11, 2006; Revised Manuscript Received July 6, 2006

ABSTRACT: All known guanidino kinases contain a conserved cysteine residue that interacts with the non-nucleophilic η_1-nitrogen of the guanidino substrate. Site-directed mutagenesis studies have shown that this cysteine is important, but not essential for activity. In human muscle creatine kinase (HMCK) this residue, Cys283, forms part of a conserved cysteine-proline-serine (CPS) motif and has a pK_a about 3 pH units below that of a regular cysteine residue. Here we employ a computational approach to predict the contribution of residues in this motif to the unusually low cysteine pK_a. We calculate that hydrogen bonds to the hydroxyl and to the backbone amide of Ser285 would both contribute ∼1 pH unit, while the presence of Pro284 in the motif lowers the pK_a of Cys283 by a further 1.2 pH units. Using UV difference spectroscopy the pK_a of the active site cysteine in WT HMCK and in the P284A, S285A, and C283S/S285C mutants was determined experimentally. The pK_a values, although consistently about 0.5 pH unit lower, were in broad agreement with those predicted. The effect of each of these mutations on the pH−rate profile was also examined. The results show conclusively that, contrary to a previous report (Wang et al. (2001) *Biochemistry 40*, 11698−11705), Cys283 is *not* responsible for the pK_a of 5.4 observed in the WT $V/K_{creatine}$ pH profile. Finally we use molecular dynamics simulations to demonstrate that, in order to maintain the linear alignment necessary for associative inline transfer of a phosphoryl group, Cys283 needs to be ionized.

Creatine kinase (CK,[11] E.C. 2.7.3.2) catalyzes the reversible transfer of the γ-phosphoryl group of ATP to creatine (Cr), forming ADP and phosphocreatine (PCr). The latter is considered to be a reservoir of "high-energy phosphate" which is able to supply ATP, the primary energy source in bioenergetics, on demand. As a result, CK plays a major role in energy homeostasis of cells with intermittently high energy requirements, such as skeletal and cardiac muscle, neurons, photoreceptors, spermatozoa, and electrocytes (*1*−*3*). CK is found in all vertebrates and exists in a variety of isoforms including the muscle, brain, and mitochondrial isozymes. The two mitochondrial isozymes, ubiquitous (Mi_u) and sarcomeric (Mi_s), can exist as dimers but are generally octameric. The subunits of the muscle (M) and brain (B) isozymes, each with a molecular mass of ∼43 kDa, form homodimers (MM, BB). In addition, they form a heterodimer (MB) which is used as a marker for myocardial infarction (*4*, *5*). In fact, cellular CK levels are perturbed in a number of human disease states including neurodegenerative diseases (*6*, *7*), muscular dystrophies (*8*), and cancer (*9*−*11*).

The catalytic mechanism of CK has undergone intensive investigation for more than 40 years. Much of the early work was focused on CK from rabbit muscle (RMCK) and has been summarized by Kenyon and Reed (*12*). More recently X-ray crystallography (*13*−*15*) and site-directed mutagenesis (*16*−*19*) have provided further evidence on those residues involved in substrate binding and catalysis. Of particular interest was the observation that two flexible loops, which provide part of the nucleotide and creatine binding sites, experience considerable conformational changes upon binding a transition-state analogue complex (TSAC) comprising creatine, nitrate, and MgADP (Figure 1). During this loop movement two residues, His66 and Asp326, move from more than 26 Å apart to within 3 Å. The active site also contained two conserved regions, the NEEDH motif (*18*) and the CPS motif (*19*). Mutation of residues in either motif resulted in greatly reduced catalytic activity. The crystallographic and mutagenesis studies have been recapitulated in a recent review (*20*).

Over the years several questions have arisen regarding the residues involved in catalysis by CK. In particular, all CK

† This work was funded in part by NSF Grant MCB 0209941 (to J.H.J.) and by NIH Grant GM44974 (to K.M.M.).

* Corresponding author. Tel: (734) 615 1787. Fax: (734) 615 3079. E-mail: mcleish@umich.edu.

‡ University of Michigan.

§ University of Iowa.

|| Present address: Department of Chemistry, University of Memphis, Memphis, TN 38152.

⊥ University of Florida.

[1] CK, creatine kinase; AK, arginine kinase; HMCK, human muscle creatine kinase; TcCK, *Torpedo californica* creatine kinase; RMCK, rabbit muscle creatine kinase; Cr, creatine; PCr, phosphocreatine; TSAC, transition-state analogue complex; CPS, cysteine-proline-serine; MES, 2-(*N*-morpholino)ethanesulfonic acid; TES, 2-[(2-hydroxy-1,1-bis[hydroxymethyl]ethyl)amino]ethanesulfonic acid; TAPS, 2-[(2-hydroxy-1,1-bis[hydroxymethyl]ethyl)amino]-1-propanesulfonic acid; DTT, dithiothreitol; HEPES, *N*-(2-hydroxyethyl)piperazine-*N*′-(2-ethanesulfonic acid); SDS PAGE, sodium dodecyl sulfate polyacrylamide gel electrophoresis; WT, wild-type; CD, circular dichroism; MD, molecular dynamics; r^2, square of the correlation coefficient.

10.1021/bi0607002 CCC: $33.50
Published on Web 08/30/2006

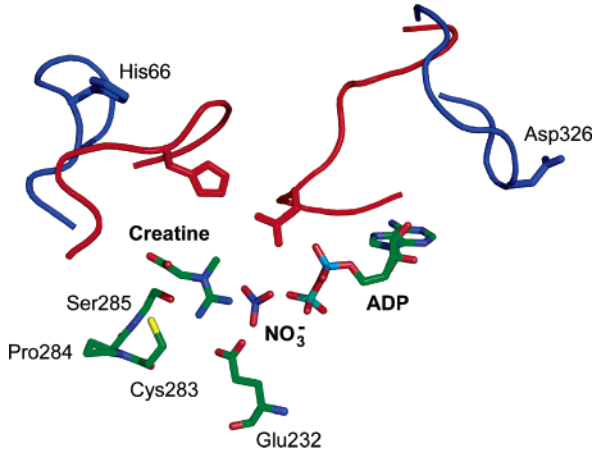

FIGURE 1: Active site of *Torpedo californica* creatine kinase bound to a transition-state analogue complex comprising creatine, nitrate and MgADP. For clarity, the only residues shown are those referred to in the text. The movement of the flexible loops is highlighted by the overlay of the loops (blue) from the TcCK:ADP complex. The figure was drawn with PyMOL (DeLano Scientific LLC) using coordinates from PDB 1VRP (*15*).

isomers were found to contain a reactive cysteine residue (*21*, *22*) and, for many years, there was considerable debate as to whether this residue was "essential". Ultimately, site-directed mutagenesis studies (*16*, *19*) showed that it was not, although an X-ray structure confirmed that it did interact with creatine within the CK active site (Figure 1) (*15*). Another intriguing question relates to the pH studies of Cook et al. (*23*) which were carried out using RMCK. The V_{Cr} pH profile revealed a single group with a p*K* around 7 whereas the V/K_{Cr} pH profile exhibited two p*K*s, of 5.6 and 7.4. It was suggested that the group with the p*K* around 7 was probably a histidine acting as an acid−base catalyst, although a lysine with a low p*K* could not be ruled out. The group with the p*K* of 5.6 must be ionized for creatine binding and was likely to be a carboxyl group (*23*). The two questions became interrelated when the "essential" cysteine residue, Cys283 in HMCK,[2] was subsequently shown by UV spectrophotometry to have a pK_a of 5.6 and, further, it was shown that a HMCK variant wherein the cysteine was replaced by serine exhibited a V/K_{Cr} pH profile lacking the lower p*K* (*19*). Taken together, these data suggested that Cys283 existed as a thiolate anion and was responsible for the p*K* of 5.4 observed in the V/K_{Cr} pH profile for HMCK (*19*). The identity of the residue responsible for the p*K* ~7 has yet to be identified.

At 5.6, the pK_a value of Cys283 is considerably perturbed from the standard pK_a value of 9.1 for cysteine residues (*24*). The factors contributing to the low pK_a value are not all immediately apparent, although it was shown that a S···OH bond between Cys283 and Ser285 (Figure 2A) contributed about 1 pH unit to the lowered pK_a value (*19*). This experimental result was in good agreement with the calculations of Naor and Jensen (*25*), who also hypothesized that the hydrogen bond between Cys283 and the amide of Ser285 would contribute approximately 1.5 pH units. Removal of these two hydrogen bonds would be expected to increase the pK_a value of Cys283 to ~8.1, which is still below the standard pK_a value for a cysteine residue.

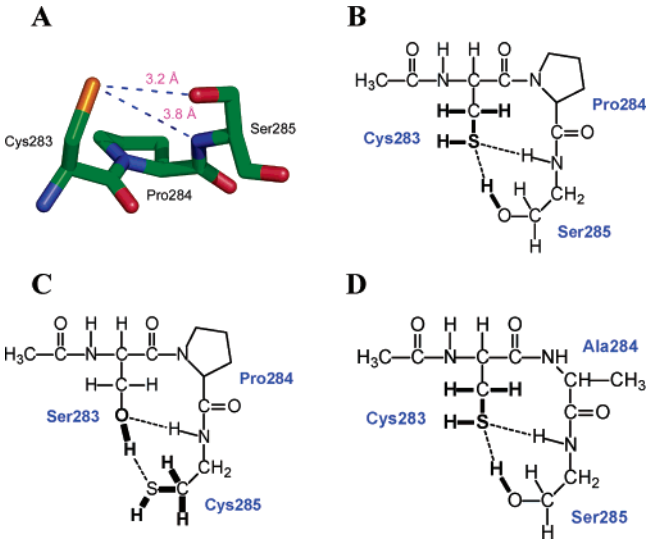

FIGURE 2: (A) The CPS motif containing Cys283 which is conserved throughout the creatine kinases. The O···S and N···S interatomic distances are both less than 4 Å. Drawn with PyMOL using coordinates from PDB 1QK1 (*30*). Panels B, C, and D are the models for the WT, C283S/S285C, and P284A variants, respectively. The OH···S and NH···S hydrogen bonds are highlighted. In each case the positions of the atoms in bold were energy minimized and the lowest energy conformational isomer is shown.

In this study we have employed a computational approach to predict the individual contributions to the pK_a of Cys283. We have then used a combination of mutagenesis and experimental techniques to (i) check the accuracy of the predicted pK_a values and (ii) demonstrate that mutations affecting the pK_a of Cys283 are not reflected in the pH−rate profile. Further we use molecular dynamics simulations to support the hypothesis that the protonation state of Cys283 plays a significant role in limiting the mobility of creatine within the active site.

EXPERIMENTAL PROCEDURES

Materials. Restriction enzymes and dNTPs were purchased from Promega or New England Biolabs. *Pfu* DNA polymerase was from Stratagene. The expression plasmids for HMCK (*26*), HMCK C283S (*19*), and HMCK S285A (*19*) were available from previous studies. Primers for mutagenesis were obtained through the University of Michigan DNA Synthesis Core Facility or were purchased from Integrated DNA Technologies. Isopropyl-β-D-thiogalactopyranoside (IPTG) was from Gold Biotechnology. Creatine, phosphocreatine, ATP, ADP, NADH, NADP, and phosphoenolpyruvate were purchased from Sigma Chemical Co. The coupling enzymes used in activity assays, pyruvate kinase, lactic dehydrogenase, hexokinase, and glucose-6-phosphate dehydrogenase, were also purchased from Sigma. All buffer salts and other reagents were of the highest quality commercially available.

Computational Methodology. The methodology employed to calculate the pK_a of the active site Cys was essentially identical to that of Naor and Jensen (*25*) and based on previous work by Li et al. (*27*). In this approach, the free energy of deprotonation of a selected residue is calculated

[2] There has been some variation in the numbering system employed for CK isozymes. The convention used here is consistent with the sequence of HMCK, including the N-terminal methionine. Thus, in this paper, Cys283 is equivalent to the Cys282 referred to in earlier studies of human and rabbit muscle CK.

using quantum chemical methods and compared to that of a reference compound. This free energy, in turn, is converted to a pK_a value. The effect of ionic strength is not included, as the ionic strength dependencies of cysteine pK_a values are not known. However, Garcia-Moreno et al. (*28*, *29*) have shown that increasing the ionic strength from ca. 10 mM (no salt added) to 100 mM shifts the pK_a of histidine residues by, at most, 0.5 pH unit. Therefore, while the spectrophotometric pK_a measurements described herein were carried out at 200 mM KCl, we do not expect that the conclusions in this paper will be greatly affected by the neglect of ionic strength dependencies in the calculations.

Protein Model Construction. Since the experimental geometries of the P284A and C283S/S285C mutants were not available, the structural models of the mutants were constructed from the wild type model (with Cys deprotonated) used by Naor and Jensen (*25*) (Figure 2B). In the case of the C283S/S285C variant the S and O atoms were interchanged (Figure 2C). This was followed by energy minimization of all atoms except the α carbons of Thr282 (represented by a methyl group in Figure 2B−D) and Ser285, and the ring atoms in Pro284. For the P284A mutant the methylene units in the proline ring were replaced by a single methyl group (Figure 2D), followed by energy minimization of all atoms except the α carbons of Thr282 and Ser285. The model uses the coordinates from PDB 1QK1 for mitochondrial (*30*) creatine kinase as the relatively low resolution (3.5 Å) structure of HMCK had been shown previously to give erroneous results (*25*).

In the acid (protonated) models, four positions of the cysteine proton (added manually) and the serine hydroxyl hydrogen atom were considered (*25*). The total free energy of the acid form was taken to be the "conformational average" of the free energies of each conformer (G_i), eq 1(*31*),

$$G = -RT \ln(\sum_i e^{-G_i/RT}) = G_0 - RT \ln[1 + \sum_{i(i>0)} e^{-\Delta G_i/RT}] \quad (1)$$

where G_0 is the lowest energy conformer, and $\Delta G_i = G_i - G_0$. In the case of the P284A mutant the position of all atoms except the α carbons of Thr282 and Ser285 were energy minimized following protonation of Cys283, while for the C283S/S285C mutant only the positions of the SH and methylene hydrogen atoms as well as the Ser285 hydroxyl hydrogen atom were energy minimized (following Naor and Jensen (*25*)).

Site-Directed Mutagenesis. Mutagenesis reactions were carried out with *Pfu* DNA polymerase and the QuikChange Site-Directed Mutagenesis Kit (Stratagene), using pETH-MCK (*26*) as the DNA template. The presence of the mutation and fidelity of the mutagenesis were confirmed by sequencing.

Expression and Purification of the HMCK Mutants. Following transformation of the appropriate plasmid into *Escherichia coli* BL21(DE3)pLysS, the proteins were expressed and purified using previously described methods (*19*) with only minor modifications. Each of the mutants exhibited an elution profile from the Blue Sepharose CL-6B column similar to that of the WT enzyme, with the protein being eluted in TES buffer (10 mM TES, 1 mM DTT, pH 8.0) containing 20 mM KCl. After further purification on a HiPrep Q column each mutant exhibited a single band on SDS PAGE.

Physical Characterization of the HMCK Mutants. Far-UV (190−240 nm) CD spectra were recorded on a Jasco J-810 spectropolarimeter at 25 °C which had been calibrated using *d*-10-camphorsulfonic acid. Cells having a path length of 0.1 cm were used and maintained at the required temperature using a Jasco PTC-423S Peltier system. Spectra were an average of 5 scans recorded with a bandwidth of 1 nm, a 0.2 nm step size, and a 1 s time constant. Thermal denaturation was monitored by changes in ellipticity at 222 nm while the cell was heated from 25 to 65 °C at 15 °C h^{-1}.

Electrospray mass spectrometry was performed on a Finnigan LCQ mass spectrometer interfaced with a Finnigan Surveyor HPLC system.

Enzyme Activity and Kinetic Parameters. The activity of HMCK was measured in both the forward and reverse directions using coupled assays as described previously (*32*). In the forward direction, i.e., creatine phosphorylation, the reaction was coupled to the reactions of pyruvate kinase and lactic dehydrogenase. A typical assay mixture contained 75 mM TAPS buffer at pH 9.0, 0.36 mM NADH, 0.36 mM phosphoenolpyruvate, 1 mM magnesium acetate, and 13 mM potassium acetate, with variable concentrations of MgATP and creatine. In the reverse direction, i.e., ADP phosphorylation, the reaction was coupled to the reactions of hexokinase and glucose-6-phosphate dehydrogenase. The assay mixture contained 75 mM HEPES buffer at pH 7.0, 5 mM glucose, 1 mM NADP, and 5 mM magnesium acetate, with variable MgADP and variable phosphocreatine. Reactions were followed by monitoring the absorbance change at 340 nm due either to bleaching of NADH or to reduction of NADP. Under these conditions CK operates by a rapid equilibrium random bi bi mechanism (*33*). The kinetic parameters were calculated using nonlinear regression analysis employing the Enzyme Kinetics module of SigmaPlot (SPSS Inc.). For some variants the K_m value for creatine was higher than its solubility in buffer solution (∼100 mM). In those instances the kinetic parameters were determined under *V/K* conditions.

pH−Rate Profiles. The pH−rate profiles for reactions in the forward and reverse directions were carried out at saturating concentrations of MgATP or MgADP, respectively (*19*). Assays were carried out at 30 °C in a constant ionic strength buffer comprising 100 mM MES, 51 mM diethanolamine, and 51 mM *N*-ethylmorpholine (*34*). Data for the pH profiles which showed a decrease in log *V* or log *V/K* with a slope of 1 as the pH was decreased were fitted to eq 2. Data for the log $V/K_{creatine}$ (V/K_{Cr}) profile, which decreased with a final slope of 2 as the pH was decreased, were fitted to eq 3. When log *V* and log *V/K* profiles decreased at both low and high pH, the data were fitted to eq 4. All curve

$$\log y = \log[C/(1 + H/K_1)] \quad (2)$$

$$\log y = \log[C/(1 + H/K_1 + H_2/K_1K_2)] \quad (3)$$

$$\log y = \log[C/(1 + H/K_1 + K_2/H)] \quad (4)$$

fitting was carried out using SigmaPlot (SPSS Inc.). In each case, *y* represents *V* or *V/K*, *C* is the pH independent value of *y*, K_1 and K_2 represent the dissociation constants for

specific groups on the enzyme, and *H* is the proton concentration.

Spectrophotometric Measurement of the Ionization of the Thiol Group of Cys283. UV absorbance spectra were recorded at 30 °C on a Cary 100 spectrophotometer (Varian) using 1.0 cm path length cuvettes. The spectra were measured in a buffer containing 1 mM phosphate, 1 mM borate, 1 mM citrate, 0.1 mM EDTA, and 0.2 M KCl. Measurements were taken over a pH range from 4 to 9, and the buffer solutions were adjusted to the appropriate pH values with HCl or NaOH. Based on an extinction coefficient (ϵ_{280}) of 37 840 M^{-1} cm^{-1} (*35*) the concentrations of HMCK and its C283S, P284A, and C283S/S285C variants were between 11 and 14 μM. The absorption differences (WT − C283S or variant − C283S) at 240 nm, as a function of pH, were fitted to the Henderson−Hasselbalch equation,

$$\epsilon_{exp} - \epsilon_{SH} = \frac{\epsilon_{S^-} - \epsilon_{SH}}{1 + 10^{pK_a - pH}} \quad (5)$$

in which ϵ_{exp} represents the experimentally determined values of ϵ_{240} of the thiol group, and ϵ_{S^-} and ϵ_{SH} are the values of ϵ_{240} for the fully deprotonated form and the fully protonated form, respectively.

Molecular Dynamic Simulations of CK Complexes. The recently solved crystal structure of TcCK bound to a TSAC (*15*) made it possible to evaluate the structural influence exerted by the different protonation states of Cys283. MD simulations of the CK complexes (the TSAC and ADP bound monomers in PDB 1VRP) at 300 K and 1 atm were carried out using the SANDER module in AMBER 8. The AMBER protein force field parameters *ff99* (*36*) were used for modeling creatine kinase. Polyphosphate parameters developed by Meagher et al. (*37*) were obtained from the AMBER parameter database along with the parameter set for organic molecules and ions. These were used for modeling ADP and NO_3^-. We developed the force field parameters (see Supporting Information) for creatine based on *gaff* (*38*), and the partial charges were calculated using the RESP methodology (*39*). The particle mesh Ewald method (*40*) was used to calculate the long-range, nonbonding electrostatic and van der Waals interactions with default settings. An appropriate number of counterions (Na^+) were placed around the CK−TSAC complexes to achieve a neutral system, which was subsequently solvated by using the TIP3P water model (*41*) in a rectangular periodic box with a distance of 10 Å from each wall to the closest solute atoms. All bonds with hydrogen atoms involved were constrained with SHAKE (*42*). The whole system then was equilibrated by using a protocol similar to that described in Cui et al. (*43*). Equilibration was then followed by production runs of 13 and 14.5 ns for the neutral and charged Cys283 complexes, respectively, using 2 fs time steps during which snapshots were collected every 2.0 ps.

RESULTS AND DISCUSSION

Calculation of pK_a values. Cys283 is part of the CPS motif (Figure 2A) which is conserved across the creatine and glycocyamine kinases. In the lombricine and arginine kinases the serine is replaced by a threonine, but the spatial arrangement of the hydrogen bonds is maintained. Using a structural model involving only Cys283, Pro284, and Ser285 (Figure 2B) and based on the coordinates of human ubiquitous mitochondrial CK (*30*), Naor and Jensen (*25*) predicted a pK_a value of 6.1 for Cys283. This was in reasonable agreement with the experimental value of 5.6 (*19*). Removal of the Ser side chain, thereby creating a model for the S285A variant, increased the calculated pK_a value to 7.2, also in good agreement with the experimental value of 6.7 obtained for this mutant (*19*). This suggests that the OH···S hydrogen bond contributes to, but is not solely responsible for, the low pK_a value of Cys283. It was proposed that further contribution may come from the hydrogen bond Cys283 makes to the backbone NH of Ser285. Additional calculations, using a model lacking Ser285, showed that this interaction contributes ~1.5 pH units to the pK_a value of Cys283 (*25*).

Table 1: Calculated and Experimental pK_a Values for Cys283 in WT and Variant Hmck

HMCK variant	thiol pK_a	
	calc	exp[a]
WT	6.2[b]	5.7 ± 0.1
P284A	7.4	6.4 ± 0.1
S285A	7.2[c]	6.7 ± 0.1[d]
C283S/S285C	7.1	7.1 ± 0.2

[a] $\Delta\epsilon_{240\ nm}$−pH data were fitted to eq 5. [b] From ref *25*. [c] From ref *25*, calculated for S285G. [d] From ref *19*.

Perhaps a better model to examine the S···NH interaction, one that can be tested both computationally and experimentally, is the C283S/S285C double mutant. The model used in the computational analysis of C283S/S285C (Figure 2C) shows that this variant retains the Ser−Cys hydrogen bond but the amide−Cys hydrogen bond has been removed. Calculations based on this model provide a pK_a value for Cys285 of 7.1 (Table 1), suggesting that the S···NH interaction lowers the pK_a of Cys283 by 0.9 pH unit.

Knowing that Pro284 is fully conserved, and that proline residues have less conformational freedom than other residues, it is conceivable that Pro284 plays a role in maintaining the interactions between Cys283 and Ser285. To test this possibility a model was prepared in which Pro284 was replaced by alanine (Figure 2D). Calculations based on this model predict a pK_a of 7.4 for Cys283 implying that Pro284 contributes more than 1 pH unit to the cysteine pK_a.

Physical Characterization of HMCK Variants. Expression levels for all proteins were similar, and each was obtained in soluble form. The presence of the mutations was confirmed by mass spectrometry (data not shown). The CD spectra and temperature-dependent unfolding profiles for the WT and mutant proteins were essentially identical (data not shown), suggesting that the mutations had little or no effect on protein folding and stability.

Steady-State Kinetic Analysis. In the initial examination of the effect of the mutations, the activities of the WT and variant HMCKs were determined in the forward direction using a standard assay mixture at pH 9.0 (Table 2). Surprisingly, given that Pro284 is conserved across the guanidino kinases, the P284A variant showed both activity and synergy in substrate binding (as evidenced by $K_m < K_d$) similar to that of the WT enzyme. The S285A variant retained about 40% of the WT activity but with reduced

Table 2: Kinetic Parameters for Reaction in the Direction of Creatine Phosphorylation[a]

HMCK variant	k_{cat} (min^{-1})	MgATP K_d (mM)	MgATP K_m (mM)	creatine K_d (mM)	creatine K_m (mM)
WT	9630 ± 215	1.0 ± 0.1	0.20 ± 0.03	80 ± 15	15 ± 1
C283S[b]	130 ± 6	nr[c]	nr	nr	222 ± 13
P284A	8860 ± 990	1.2 ± 0.1	0.50 ± 0.03	66 ± 6	26 ± 1
S285A	4270 ± 630	1.2 ± 0.1	2.3 ± 0.3	170 ± 45[d]	320 ± 60[d]
S285C	19 ± 2	1.5 ± 0.6	1.4 ± 0.3	68 ± 31	70 ± 25
C283S/S285C	795 ± 150	1.4 ± 0.1	4.3 ± 1.3	173 ± 30[d]	490 ± 110[d]

[a] Kinetic constants are shown ± SEM. [b] Data from ref *19*. [c] Not reported. [d] Kinetic data obtained at creatine concentrations below 100 mM.

Table 3: Kinetic Parameters for Reaction in the Direction of adp Phosphorylation[a]

HMCK variant	k_{cat} (min^{-1})	MgADP K_d (μM)	MgADP K_m (μM)	phosphocreatine K_d (mM)	phosphocreatine K_m (mM)
WT	28040 ± 990	84 ± 12	31 ± 5	3.6 ± 0.1	1.3 ± 0.1
C283S[b]	60 ± 2	nr[c]	nr	nr	3.4 ± 0.2
P284A	32350 ± 1080	72 ± 8	60 ± 6	3.1 ± 0.4	2.6 ± 0.2
S285A	614 ± 10	26 ± 4	6.7 ± 0.7	4.4 ± 0.7	1.1 ± 01
S285C	29 ± 2	56 ± 9	43 ± 7	4.9 ± 1.1	3.7 ± 0.3
C283S/S285C	38 ± 1	69 ± 9	7 ± 2	11 ± 3	1.1 ± 0.1

[a] Kinetic constants are shown ± Se. [b] Data from ref *19*. [c] Not reported.

affinity for creatine as well as a loss of synergy in substrate binding. By contrast, the S285C variant had WT-like affinity for substrates, but a 500-fold decrease in k_{cat} value. Much of the catalytic activity was recovered in the C283S/S285C double mutant which showed only a 12-fold decrease in k_{cat}. However this was accompanied by a 30-fold increase in value of K_m for creatine, underlining the importance of the thiolate anion in the binding of guanidino substrates.

The kinetic data for reaction at pH 7.0 in the reverse direction are provided in Table 3. Overall the results mirrored those for reaction in the forward direction with the major exceptions being the S285A and C283S/S285C variants. The k_{cat} value of the S285A was only 2% of the wild-type value (cf. 40% in the forward reaction). For C283S/S285C the K_m value for phosphocreatine was similar to that of the WT enzyme whereas the K_m value for creatine was 30-fold higher than that of the WT. More surprisingly, there was a 3-fold increase in the synergy of substrate binding for C283S/S285C in the reverse direction compared to a 15-fold loss in the forward reaction. The reasons for this increase are not clear.

Spectrophotometric Determination of the pK_a Value of Cys283. It is possible to determine the ionization state of a thiol group spectrophotometrically by comparing the difference in UV absorbance between the dissociated form and the undissociated form. The latter has negligible absorbance at 240 nm whereas the thiolate anion has a characteristic UV absorption band centered around 240 nm with an extinction coefficient of about 4000 M^{-1} cm^{-1} (*44*, *45*). Given that many groups on a protein absorb at this wavelength, and that some of the absorbance may be pH-dependent, it is necessary to compare the UV spectrum of a protein containing the thiol group of interest to the spectrum of the same protein in which the thiol group is absent (*46*, *47*). Presumably, any absorbance observed in the difference spectrum will arise from the thiolate anion.

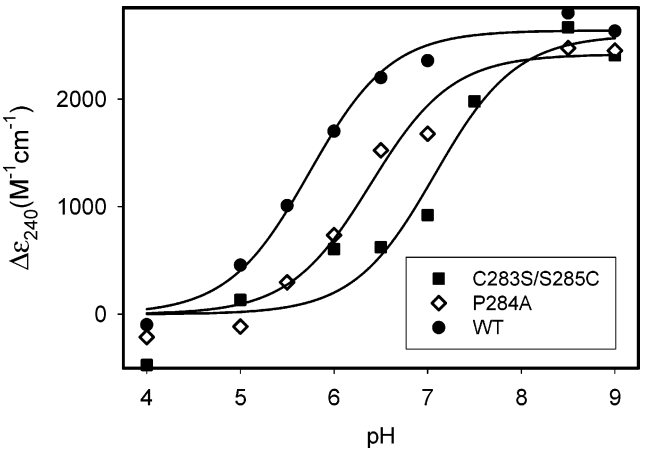

FIGURE 3: Determination of the pK_a of the thiol group of Cys283. The absorbance spectrum was obtained for each protein (11−14 μM) in a buffer containing 1 mM citrate, 1 mM borate, 1 mM phosphate, 0.2 M KCl, and 0.1 mM EDTA. The differences in the molar extinction coefficient at 240 nm ($\Delta\epsilon_{240}$) between the HMCK variants and HMCK C283S are shown as a function of pH. The symbols are the experimentally determined data, while the solid lines show the fits of the data to eq 5. The fits provide p*K*s of 5.7, 6.4, and 7.1 for the WT, P284A, and C283S/S285C variants, respectively.

The UV absorbance spectra of wild-type HMCK and its C283S variant were measured over a pH range of 4 to 9. The differences between the molar extinction coefficients at 240 nm for the two proteins ($\Delta\epsilon_{240}$) as a function of pH are presented in Figure 3. These data, when fitted to the Henderson−Hasselbalch equation (eq 5), provided a pK_a for Cys283 (in the wild-type enzyme) of 5.7 ± 0.1. This is consistent with the value of 5.6 ± 0.1 determined in a previous study (*19*) and demonstrates that the method is reproducible between enzyme preparations. The $\Delta\epsilon_{240}$ for the P284A and C283S, as well as the C283S/S285C and C283S, variants was determined over the same pH range (Figure 3). After the data were fitted to eq 5, the pK_a of Cys283 in the HMCK P284A variant was found to be 6.4 ± 0.1, and that of Cys285 in C283S/S285C was 7.1 ± 0.2. While the latter is in excellent agreement with the calculated value, the experimental pK_a for the P284A variant was almost a full pH unit lower than the calculated value.

From a computational point of view, the calculated pK_a values are broadly consistent with the UV difference results (Table 1). Experimentally, WT HMCK has a pK_a value of 5.7 ± 0.1, whereas the calculated value is 6.1 (*25*). The C283S/S285C value is 7.1 in both experiment and calculation. The only significant difference occurs with the P284A variant, where the experimental value is 6.4 and the calculated value is 7.4. It may be argued that this is a sizable difference, perhaps due to changes brought about by the mutation that are not reflected in this model. Nonetheless it should be recognized that both calculation and experiment show that Pro284 makes a substantial contribution to the pK_a of Cys283, 1.2 and 0.7 pH units, for calculation and experiment, respectively. Overall, the experimental results seem to validate the pK_a prediction methodology and confirm that the S···OH and S···NH interactions, as well as the conformational restraint provided by Pro284, are the major determinants of the abnormally low pK_a of Cys283.

pH Profiles for HMCK Variants for Reaction in the Forward Direction. Previous studies on both RMCK (*23*) and HMCK (*19*) have shown that the pH profile of k_{cat}/K_m for creatine (V/K_{Cr}) exhibits two p*K*s at around 5.5 and 7−7.5. When it was shown that Cys283 exists as the thiolate ion, and that the C283S variant appeared to "lose" the p*K* at 5.5, the lower p*K* was ascribed to Cys283 (*19*). However, upon reflection, there were some anomalies which brought this assignment into question. First and foremost, the *V*/*K* pH profile for phosphocreatine (V/K_{PCr}) for WT HMCK has p*K*s at 5.8 and 7.5, while that for the C283S variant has p*K*s at 5.8 and 7.8 (*19*). The X-ray data indicate that both creatine and phosphocreatine will have similar interactions with Cys283 (*15*), and it is hard to envision that CK has evolved to have two active site residues, both with p*K*s around 5.5, that play different roles in the forward and reverse direction. Yet, if the "missing" p*K* in the C283S V/K_{Cr} profile is correctly attributed to Cys283, this is the logical corollary. Fortunately, the UV difference study provided us with the means to address this conundrum.

In the HMCK S285A variant, Cys283 was shown spectrophotometrically to have a pK_a of 6.7 ± 0.1 (*19*). This means that the hydrogen bond between Cys283 and Ser285 (Figure 2a) must lower the cysteine pK_a value by ~1.0 pH unit (Table 1 (*19*)). On that basis, if the lower p*K* in the WT V/K_{Cr} profile was attributed to Cys283, it would be reasonable to assume that the analogous p*K* in the S285A profile would also exhibit an increase of ~1 pH unit. However, as shown in Figure 4A, the S285A pH profile exhibited two p*K*s, at pH values of 5.5 and 6.9 ($r^2 = 0.995$), similar to those of the WT enzyme (Table 4). The lack of any increase clearly indicates that, at least for S285A, Cys283 is *not* responsible for the lower p*K*. It should be noted that the poor solubility of creatine limits its concentration in an assay to less than 100 mM. This makes it difficult to obtain meaningful kinetic data for S285A which has a high K_m value for creatine (320 mM, Table 2). To circumvent this problem, pH−rate data for S285A were obtained under *V*/*K* conditions, i.e., where [creatine] ≪ K_m. This ensures that the k_{cat}/K_m data are accurate but does not permit the measurement of k_{cat} alone.

This observation prompted a reevaluation of the initial data for the C283S variant which were not obtained under *V*/*K* conditions, even though the K_m values for creatine were in excess of 100 mM. The analysis showed that the earlier data could be fitted almost equally well to equations for both one and two p*K* systems, with the latter providing p*K*s of 5.1 and 6.3 (data not shown). In an attempt to clarify this issue new experimental data were obtained for the C283S variant, this time under *V*/*K* conditions, with considerable effort being expended in obtaining accurate data at lower pH values. The new V/K_{Cr} profile for C283S is shown in Figure 4B. This profile verifies the presence of two p*K*s, at pH values of 5.5 ± 0.2 and 6.4 ± 0.1 ($r^2 = 0.994$; Table 4). By comparison, fitting the data to a single p*K* provided a value of 6.6 ± 0.1 ($r^2 = 0.979$). The fit to a single p*K* was passable, but, unlike that for the data of Wang et al. (*19*), the r^2 value was clearly lower than that of the two p*K* fit (Figure 4B). The two curves in Figure 2B emphasize the fact that the fit to either one or two p*K*s relies to a large extent on results obtained at the lowest pH values where it is most challenging to obtain consistent data. As reported earlier (*19*), at low pH the coupled assay is made difficult by the degradation of NADH and the coupling enzymes. Further, the k_{cat} value of C283S, even under optimal conditions, is 30−70-fold lower than the other variants used in this study, which makes these measurements even more problematic. When these issues are combined with the creatine solubility problem, it is not

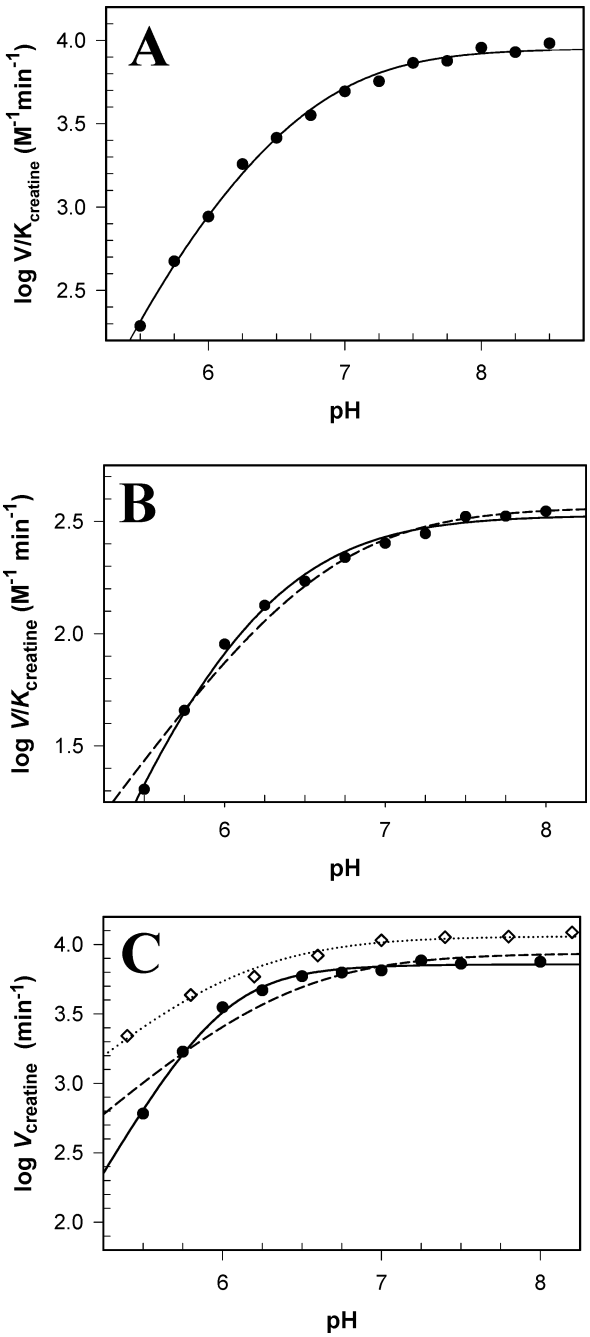

FIGURE 4: Plots showing the pH dependence of V_{max}/K_m for the (A) HMCK S285A and (B) C283S variants, and (C) the pH dependence of V_{max} for P284A for reaction in the forward direction. All the assays were carried out in a constant ionic strength buffer (*34*) as described in Experimental Procedures. The symbols are the experimentally determined data. In panel A the solid line shows the fit of the data to eq 3 which provides two p*K*s of 5.5 and 6.9 ($r^2 = 0.995$). In panel B the solid line is the fit of the data to eq 3 which affords two p*K*s of 5.5 and 6.4 ($r^2 = 0.994$), whereas the dashed line is the fit of the data to eq 2 which provides a single p*K* of 6.6 ($r^2 = 0.979$). In panel C the solid line is the fit of the data to eq 3 which gives two p*K*s of 5.5 and 6.5 ($r^2 = 0.993$). Fitting the data to eq 2 (dashed line) results in a single p*K* of 6.4 ($r^2 = 0.910$). Data from ref *19* for the WT enzyme (open diamonds, dotted line) is included for comparative purposes.

Table 4: Summary of Data Obtained from pH−Rate Profiles for the Forward Reaction[a]

	V_{Cr}		V/K_{Cr}	
HMCK variant	pK_1	pK_2	pK_1	pK_2
WT	*b*	6.1 ± 0.1	5.4 ± 0.2	6.7 ± 0.1
C283S	nd[c]	nd	5.5 ± 0.1	6.4 ± 0.1
S285A	nd	nd	5.5 ± 0.1	6.9 ± 0.1
C283S/S285C	nd	nd	5.5 ± 0.1	6.9 ± 0.1
P284A	5.5 ± 0.3	6.5 ± 0.3	5.3 ± 0.2	6.8 ± 0.1

[a] Unless noted, pH−rate data were fitted to eq 3. [b] This pK was not observed, and the data were fitted to eq 2. [c] Not determined as data were obtained under V/K conditions.

entirely surprising that the results of Wang et al. (*19*) were open to erroneous interpretation.

The pK_a values for the active site thiol in the P284A and C283S/S285C variants, as determined by UV spectrophotometry, were also quite different from that of WT HMCK. These differences permitted us to use the latter variants as further controls. In both instances pK values similar to those of the WT enzyme were observed in the V/K_{Cr} profile (Table 4), lending support to the suggestion that the pK_a of Cys283 is not reflected in that profile. The P284A variant has almost WT activity, and its K_m value for creatine is relatively low (Table 2). Initially this was thought to be an advantage as it would enable us to determine a k_{cat} pH profile. However, ultimately, P284A provided an anomalous result in that its pH profile for k_{cat} in the forward reaction (Figure 4C) clearly shows two pKs, unlike that of the WT enzyme, which shows only one. One interpretation of this result is that the P284A mutation causes a shift in the k_{cat} profile toward higher pH values. This implies that the WT k_{cat} profile also has two pKs, but that our assay conditions are such that the second pK cannot be observed. Given that both the k_{cat} and V/K_{PCr} profiles for the reverse direction have two pKs (*19*, *23*), it was always somewhat surprising for the forward k_{cat} profile to have only one pK (*19*), so this explanation would seem to have some merit.

Molecular Dynamic Simulations of CK Complexes. Generally it is accepted that a glutamic acid residue acts as the catalytic base in both creatine (*18*) and arginine (*48*) kinases, if indeed one is required (*49*). Why then is Cys283 unprotonated? It has been proposed that it could enhance catalytic activity by drawing positive charge away from the nucleophilic guanidinium $N_{\eta 2}$ or by constraining the position of the guanidinium of the substrate (*48*). To explore this question we carried out individual MD simulations of the solvated CK−TSAC complex containing either a neutral or a charged Cys283 residue. These were carried out at constant temperature (300 K) and allowed us to directly examine the impact of the protonation state of Cys283 on the structure and dynamics of the complex in solution. The protein backbone root-mean-square deviations (rmsd) were calculated against the crystal conformation (Figure 5a), and the final conformations of the two simulated CK−TSAC structures are presented in Figure 6. In both simulations the backbone conformation slowly drifted away from that in the crystal environment during the first 5 ns.

The CK−TSAC structure (*15*) implies coordinated N-terminal and C-terminal domain motions that are connected to the substrate binding and release. This has been supported by the anti-correlated fluctuations observed in the first low-

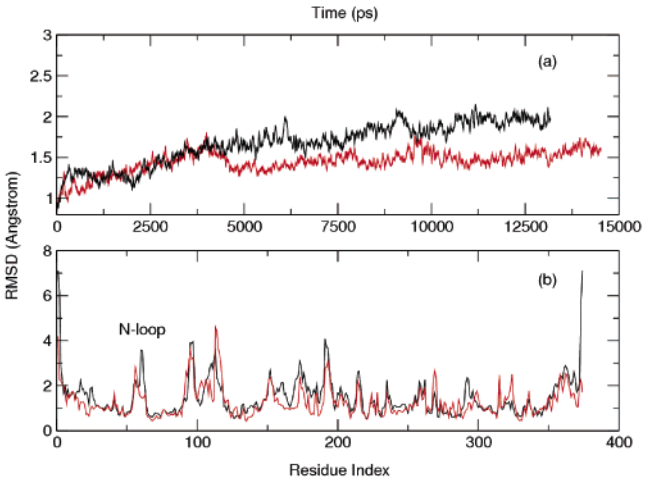

FIGURE 5: For the MD simulations of the Cys283−neutral (black) and Cys283−anion (red) complexes, (a) the backbone root-mean-square deviations (in Å) were plotted against the simulation length (in picoseconds) averaged every 20 ps, and (b) the average residue backbone root-mean-square deviations (in Å) were calculated for all protein residues from the last 10 ns of each MD simulation. The binding loop from the N-terminal domain (residue 60 to 70) is noted as N-loop.

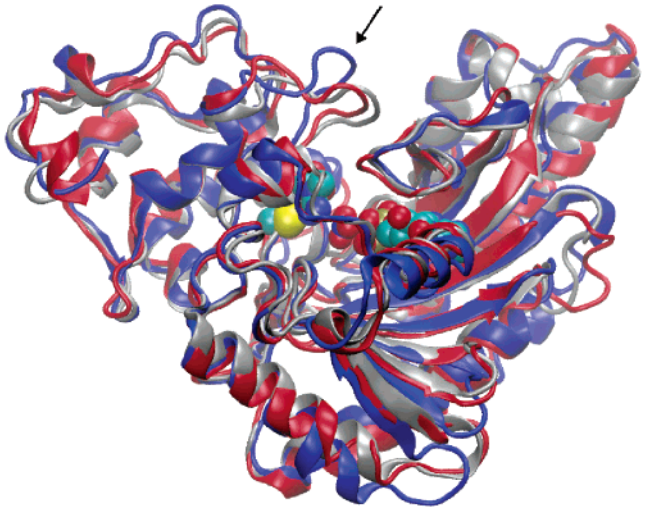

FIGURE 6: The final MD snapshots of creatine kinase sampled during the MD simulations are shown as colored ribbon diagrams (red, Cys283−anion; blue, Cys283−neutral). The side chain of Cys283, creatine, nitrate, and ADP are represented as van der Waals spheres colored by element types (hydrogen atoms are excluded). These are superimposed on the crystal conformation of CK−TSAC (gray). The opening of the N-terminal loop is highlighted. MD snapshots taken after 2, 4, 6, 8, 10, 12, and 14 ns are available as Supporting Information.

frequency mode calculated using Gaussian Network Model (data not shown). Therefore it is not surprising that the most noticeable conformational changes occur in these two regions, as the hinge region is relatively more stable. Despite the fact that the overall structures are similar, a significant difference is evident in the subsequent trajectories in that the Cys283−neutral complex exhibits a larger backbone rmsd compared to the Cys283−anion complex, particularly in the active site loop region (residue 60 to 70) of the N-terminal domain (Figure 5b and Figure 6). The noticeable opening of this catalytically significant loop (*50*) is likely the consequence of the weakened creatine binding. The latter is illustrated in the mass density plot of the creatine residue in

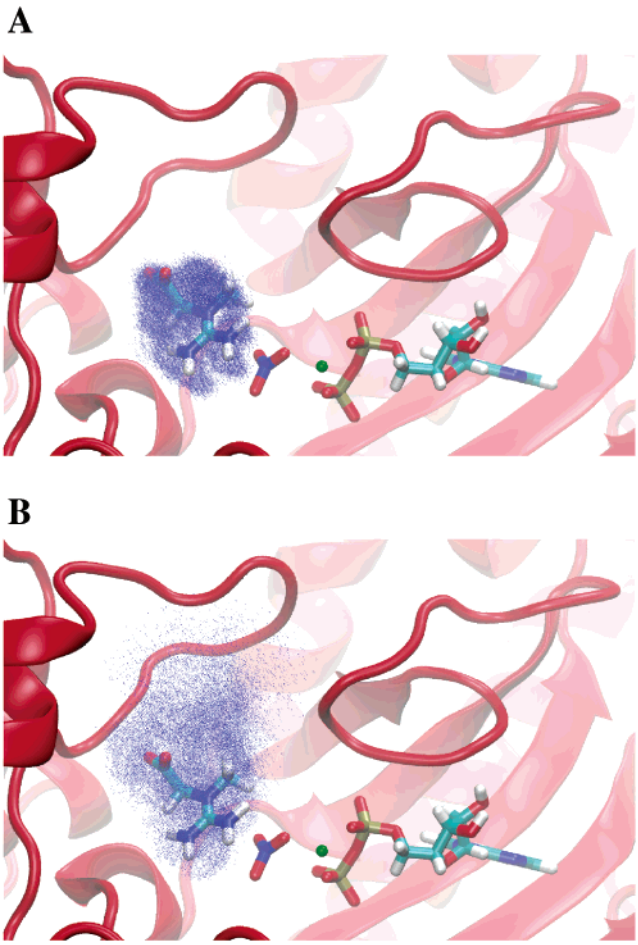

FIGURE 7: Mass densities of creatine sampled during the two MD simulations plotted at the same isosurface value against the crystal conformation of CK−TSAC (A, Cys283−anion; B, Cys283−neutral). Creatine, nitrate, magnesium, and ADP are shown as licorice.

the active site during the MD simulations (Figure 7). In the Cys283−anion complex the creatine residue maintains a well-defined position in the tightly enclosed binding pocket. By contrast, in the Cys283−neutral complex, creatine rotates almost freely during the MD simulation. One consequence of this movement would be the disruption of the interaction between Ile69 and the methyl group of creatine, possibly leading to the opening of the N-terminal loop. This interaction has been shown previously to be important for CK catalysis (*51*). Another result of the creatine rotation is that the linear arrangement of creatine, nitrate, and the β-phosphate of ADP, thought to mimic phosphoryl group transfer in the transition state of the CK reaction, is lost. Interestingly, the hydrogen-bonding network of creatine with surrounding residues observed during the MD simulation of the Cys283−anion complex was different from that found in the crystal structure of CK−TSAC. This is likely caused by a gauche$^-$−gauche$^+$ transition of the carboxylate group of creatine, which was able to form hydrogen bonds not only with Val72 but also with Ser285. Cys283 preferred to form hydrogen bonds with the guanidino group of creatine, having little contact with the backbone amide proton of Ser285. Taken together, the results support the early suggestions of Zhou et al. (*48*) that the primary role of the active site cysteine of the phosphagen kinases is to constrain the position of the substrate guanidinium, although it may also accept a hydrogen bond from the substrate.

CONCLUSIONS

We have used UV difference spectroscopy to confirm that, at 5.7 ± 0.1, the pK_a of HMCK Cys283 is about 3 pH units below that of a regular cysteine residue. The computational methodology of Naor and Jensen (*25*) was used to predict that hydrogen bonds to the hydroxyl and to the backbone NH of Ser285 would both contribute ~1 pH unit to the abnormal pK_a of Cys283. Cysteine pK_a values determined experimentally for the S284A and C283S/S285C variants confirmed these predictions. In addition, we have also shown experimentally that the presence of Pro284 in the CPS motif lowers the Cys283 pK_a by a further 0.7 pH unit. Overall, the utility of this methodology in thiol pK_a predictions has been validated.

Previously it has been suggested that Cys283 is the neutral acid responsible for the pK of 5.5 in the V/K_{Cr} pH profile (*19*). We have unambiguously shown that this is not the case, and that this pK is still observed even with variants in which the thiol pK_a has increased by 1.5 pH units. Further, we have demonstrated that, upon reexamination, the V/K_{Cr} profile for the C283S variant indeed contains the pK of 5.5.

Finally, MD simulations indicate that the prime role of Cys283 is to constrain the position of the guanidinium group of the substrate, and that this does not occur if the cysteine is protonated. It is likely that the requirement for an ionized active site cysteine obtains across the entire family of guanidino kinases.

SUPPORTING INFORMATION AVAILABLE

A table of force field parameters developed for creatine and a figure containing snapshots of creatine kinase taken during the MD simulations. This material is available free of charge via the Internet at http://pubs.acs.org.

REFERENCES

1. Wallimann, T., Wyss, M., Brdiczka, D., Nicolay, K., and Eppenberger, H. M. (1992) Intracellular compartmentation, structure and function of creatine kinase isoenzymes in tissues with high and fluctuating energy demands: the 'phosphocreatine circuit' for cellular energy homeostasis, *Biochem. J. 281*, 21−40.
2. Schlattner, U., Forstner, M., Eder, M., Stachowiak, O., Fritz-Wolf, K., and Wallimann, T. (1998) Functional aspects of the X-ray structure of mitochondrial creatine kinase: a molecular physiology approach, *Mol. Cell. Biochem. 184*, 125−140.
3. Wyss, M., and Kaddurah-Daouk, R. (2000) Creatine and creatinine metabolism, *Physiol. Rev. 80*, 1107−1213.
4. Apple, F. S. (1989) Diagnostic use of CK-MM and CK-MB isoforms for detecting myocardial infarction, *Clin. Lab. Med. 9*, 643−654.
5. Apple, F. S. (1999) Creatine kinase isoforms and myoglobin: early detection of myocardial infarction and reperfusion, *Coron. Art. Dis. 10*, 75−79.
6. Aksenova, M. V., Aksenov, M. Y., Payne, R. M., Trojanowski, J. Q., Schmidt, M. L., Carney, J. M., Butterfield, D. A., and Markesbery, W. R. (1999) Oxidation of cytosolic proteins and expression of creatine kinase BB in frontal lobe in different neurodegenerative disorders, *Dement. Geriatr. Cogn. Disord. 10*, 158−165.
7. David, S., Shoemaker, M., and Haley, B. E. (1998) Abnormal properties of creatine kinase in Alzheimer's disease brain: correlation of reduced enzyme activity and active site photolabeling with aberrant cytosol-membrane partitioning, *Brain Res. Mol. Brain Res. 54*, 276−287.

8. Ozawa, E., Hagiwara, Y., and Yoshida, M. (1999) Creatine kinase, cell membrane and Duchenne muscular dystrophy, *Mol. Cell. Biochem. 190*, 143−151.
9. Zarghami, N., Giai, M., Yu, H., Roagna, R., Ponzone, R., Katsaros, D., Sismondi, P., and Diamandis, E. P. (1996) Creatine kinase BB isoenzyme levels in tumour cytosols and survival of breast cancer patients, *Br. J. Cancer 73*, 386−390.
10. Delahunt, B., Lewis, M. E., Pringle, K. C., Wiltshire, E. J., and Crooke, M. J. (2001) Serum creatine kinase levels parallel the clinical course for rhabdomyomatous Wilms tumor, *Am. J. Clin. Pathol. 116*, 354−359.
11. Huddleston, H. G., Wong, K. K., Welch, W. R., Berkowitz, R. S., and Mok, S. C. (2005) Clinical applications of microarray technology: creatine kinase B is an up-regulated gene in epithelial ovarian cancer and shows promise as a serum marker, *Gynecol. Oncol. 96*, 77−83.
12. Kenyon, G. L., and Reed, G. H. (1983) Creatine kinase: structure-activity relationships, *Adv. Enzymol. Relat. Areas Mol. Biol. 54*, 367−426.
13. Fritz-Wolf, K., Schnyder, T., Wallimann, T., and Kabsch, W. (1996) Structure of mitochondrial creatine kinase, *Nature 381*, 341−345.
14. Rao, J. K., Bujacz, G., and Wlodawer, A. (1998) Crystal structure of rabbit muscle creatine kinase, *FEBS Lett. 439*, 133−137.
15. Lahiri, S. D., Wang, P.-F., Babbitt, P. C., McLeish, M. J., Kenyon, G. L., and Allen, K. N. (2002) The 2.1 Å structure of *Torpedo californica* creatine kinase complexed with the ADP-Mg^{2+}-NO_3^--creatine transition-state analogue complex, *Biochemistry 41*, 13861−13867.
16. Furter, R., Furter-Graves, E. M., and Wallimann, T. (1993) Creatine kinase: the reactive cysteine is required for synergism but is nonessential for catalysis, *Biochemistry 32*, 7022−7029.
17. Chen, L. H., Borders, C. L., Jr., Vasquez, J. R., and Kenyon, G. L. (1996) Rabbit muscle creatine kinase: consequences of the mutagenesis of conserved histidine residues, *Biochemistry 35*, 7895−7902.
18. Cantwell, J. S., Novak, W. R., Wang, P. F., McLeish, M. J., Kenyon, G. L., and Babbitt, P. C. (2001) Mutagenesis of two acidic active site residues in human muscle creatine kinase: implications for the catalytic mechanism, *Biochemistry 40*, 3056−3061.
19. Wang, P. F., McLeish, M. J., Kneen, M. M., Lee, G., and Kenyon, G. L. (2001) An unusually low pK_a for Cys282 in the active site of human muscle creatine kinase, *Biochemistry 40*, 11698−11705.
20. McLeish, M. J., and Kenyon, G. L. (2005) Relating structure to mechanism in creatine kinase, *Crit. Rev. Biochem. Mol. Biol. 40*, 1−20.
21. Mahowald, T. A. (1965) The amino acid sequence around the "reactive" sulfhydryl groups in adenosine triphosphocreatine phosphotransferase, *Biochemistry 4*, 732−740.
22. Fedosov, S. N., and Belousova, L. V. (1988) Effect of oligomerization on the properties of essential SH-groups of mitochondrial creatine kinase, *Biokhimiya 53*, 550−564.
23. Cook, P. F., Kenyon, G. L., and Cleland, W. W. (1981) Use of p*H* studies to elucidate the catalytic mechanism of rabbit muscle creatine kinase, *Biochemistry 20*, 1204−1210.
24. Harris, T. K., and Turner, G. J. (2002) Structural basis of perturbed pKa values of catalytic groups in enzyme active sites, *IUBMB Life 53*, 85−98.
25. Naor, M. M., and Jensen, J. H. (2004) Determinants of cysteine pK_a values in creatine kinase and α1-antitrypsin, *Proteins: Struct., Funct., Bioinf. 57*, 799−803.
26. Chen, L. H., White, C. B., Babbitt, P. C., McLeish, M. J., and Kenyon, G. L. (2000) A comparative study of human muscle and brain creatine kinases expressed in *Escherichia coli*, *J. Protein Chem. 19*, 59−66.
27. Li, H., Hains, A. W., Everts, J. E., Robertson, A. D., and Jensen, J. H. (2002) The prediction of protein pK_as using QM/MM: The pK_a of lysine 55 in turkey ovomucoid third domain, *J. Phys. Chem. B 106*, 3486−3494.
28. Kao, Y. H., Fitch, C. A., Bhattacharya, S., Sarkisian, C. J., Lecomte, J. T. J., and Garcia-Moreno, B. (2000) Salt effects on ionization equilibria of histidines in myoglobin, *Biophys. J. 79*, 1637−1654.
29. Lee, K. K., Fitch, C. A., Lecomte, J. T. J., and Garcia-Moreno, B. (2002) Electrostatic effects in highly charged proteins: Salt sensitivity of pK_a values of histidines in staphylococcal nuclease, *Biochemistry 41*, 5656−5667.
30. Eder, M., Fritz-Wolf, K., Kabsch, W., Wallimann, T., and Schlattner, U. (2000) Crystal structure of human ubiquitous mitochondrial creatine kinase, *Proteins 39*, 216−225.
31. McQuarrie, D. M. (1973) *Statistical Thermodynamics*, University Science Books, Mill Valley, CA.
32. Wang, P. F., Novak, W. R. P., Cantwell, J. S., Babbitt, P. C., McLeish, M. J., and Kenyon, G. L. (2002) Expression of *Torpedo californica* creatine kinase in *Escherichia coli* and purification from inclusion bodies, *Protein Expression Purif. 26*, 89−95.
33. Morrison, J. F., and James, E. (1965) The mechanism of the reaction catalyzed by adenosine triphosphate-creatine phosphotransferase, *Biochem. J. 97*, 37−52.
34. Ellis, K. J., and Morrison, J. F. (1982) Buffers of constant ionic strength for studying p*H*-dependent processes, *Methods Enzymol. 87*, 405−426.
35. Noda, L., Kuby, S. A., and Lardy, H. (1954) *Methods Enzymol. 2*, 605−610.
36. Wang, J. M., Cieplak, P., and Kollman, P. A. (2000) How well does a restrained electrostatic potential (RESP) model perform in calculating conformational energies of organic and biological molecules?, *J. Comput. Chem. 21*, 1049−1074.
37. Meagher, K., Redman, L., and Carlson, H. (2003) Development of polyphosphate parameters for use with the AMBER force field, *J. Comput. Chem. 24*, 1016−1025.
38. Wang, J., Wolf, R. M., Caldwell, J. W., Kollman, P. A., and Case, D. A. (2004) Development and testing of a general AMBER force field, *J. Comput. Chem. 25*, 1157−1174.
39. Cieplak, P., Cornell, W. D., Bayly, C., and Kollman, P. A. (1995) Application of the multimolecule and multiconformational RESP methodology to biopolymers−charge derivation for DNA, RNA, and proteins, *J. Comput. Chem. 16*, 1357−1377.
40. Darden, T., York, D., and Pedersen, L. (1993) Particle mesh Ewald−an N.log(N) method for Ewald sums in large systems, *J. Chem. Phys. 98*, 10089−10092.
41. Jorgensen, W. L., Chandrasekhar, J., Madura, J. D., Impey, R. W., and Klein, M. L. (1983) Comparison of simple potential functions for simulating liquid water, *J. Chem. Phys. 79*, 926−935.
42. Daan Frenkel, B. S. (2002) *Understanding molecular simulation: From algorithms to applications*, 2nd ed., Vol. 1, Academic Press, San Diego.
43. Cui, G., Wang, B., and Merz, K. M., Jr. (2005) Computational studies of the farnesyltransferase ternary complex part I: substrate binding, *Biochemistry 44*, 16513−16523.
44. Noda, L., Kuby, S. A., and Lardy, H. (1953) Properties of thiolesters: kinetics of hydrolysis in dilute aqueous media, *J. Am. Chem. Soc. 75*, 913−917.
45. Polgár, L. (1974) Spectrophotometric determination of mercaptide ion, an activated form of SH-group in thiol enzymes, *FEBS Lett. 38*, 187−190.
46. Grauschopf, U., Winther, J. R., Korber, P., Zander, T., Dallinger, P., and Bardwell, J. C. (1995) Why is DsbA such an oxidizing disulfide catalyst?, *Cell 83*, 947−955.
47. Lo Bello, M., Parker, M. W., Desideri, A., Polticelli, F., Falconi, M., Del Boccio, G., Pennelli, A., Federici, G., and Ricci, G. (1993) Peculiar spectroscopic and kinetic properties of Cys-47 in human placental glutathione transferase. Evidence for an atypical thiolate ion pair near the active site, *J. Biol. Chem. 268*, 19033−19038.
48. Zhou, G., Somasundaram, T., Blanc, E., Parthasarathy, G., Ellington, W. R., and Chapman, M. S. (1998) Transition state structure of arginine kinase: implications for catalysis of bimolecular reactions, *Proc. Natl. Acad. Sci. U.S.A. 95*, 8449−8454.
49. Pruett, P. S., Azzi, A., Clark, S. A., Yousef, M. S., Gattis, J. L., Somasundaram, T., Ellington, W. R., and Chapman, M. S. (2003) The putative catalytic bases have, at most, an accessory role in the mechanism of arginine kinase, *J. Biol. Chem. 278*, 26952−26957.
50. Wang, P.-F., Flynn, A. D., McLeish, M. J., and Kenyon, G. L. (2005) Loop movement and catalysis in creatine kinase, *IUBMB Life 57*, 355−362.
51. Novak, W. R. P., Wang, P.-F., McLeish, M. J., Kenyon, G. L., and Babbitt, P. C. (2004) Isoleucine 69 and valine 325 form a specificity pocket in human muscle creatine kinase, *Biochemistry 43*, 13766−13774.

BI0607002